THE JOURNAL OF PHYSICAL CHEMISTRY A

Article

pubs.acs.org/JPCA

Hydration of the Sulfuric Acid−Methylamine Complex and Implications for Aerosol Formation

Danielle J. Bustos, Berhane Temelso, and George C. Shields*

Dean's Office, College of Arts and Sciences, and Department of Chemistry, Bucknell University, Lewisburg, Pennsylvania 17837, United States

Supporting Information

ABSTRACT: The binary H_2SO_4−H_2O nucleation is one of the most important pathways by which aerosols form in the atmosphere, and the presence of ternary species like amines increases aerosol formation rates. In this study, we focus on the hydration of a ternary system of sulfuric acid (H_2SO_4), methylamine (NH_2CH_3), and up to six waters to evaluate its implications for aerosol formation. By combining molecular dynamics (MD) sampling with high-level ab initio calculations, we determine the thermodynamics of forming $H_2SO_4(NH_2CH_3)(H_2O)_n$, where n = 0−6. Because it is a strong acid−base system, H_2SO_4−NH_2CH_3 quickly forms a tightly bound HSO_4^-−$NH_3CH_3^+$ complex that condenses water more readily than H_2SO_4 alone. The electronic binding energy of H_2SO_4−NH_2CH_3 is −21.8 kcal mol^{-1} compared with −16.8 kcal mol^{-1} for H_2SO_4−NH_3 and −12.8 kcal mol^{-1} for H_2SO_4−H_2O. Adding one to two water molecules to the H_2SO_4−NH_2CH_3 complex is more favorable than adding to H_2SO_4 alone, yet there is no systematic difference for $n \geq 3$. However, the average number of water molecules around H_2SO_4−NH_2CH_3 is consistently higher than that of H_2SO_4, and it is fairly independent of temperature and relative humidity.

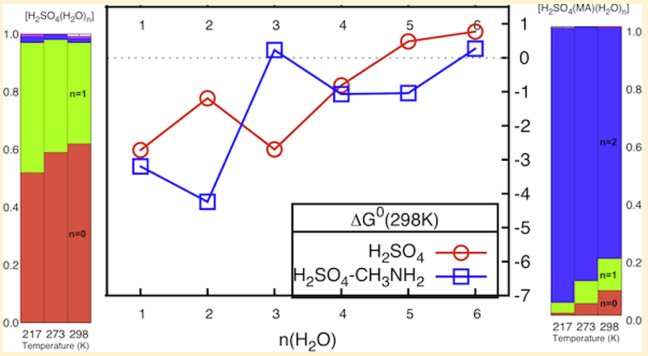

1. INTRODUCTION

Atmospheric aerosols, particulates suspended in air, affect the global climate directly and indirectly.[1] Their net cooling effect of −1.2 ± 1 W m^{-2} is almost comparable to the warming effect of greenhouse gases, 1.7 ± 0.2 W m^{-2}.[2] One of the most important vapors leading to the formation of secondary aerosols is sulfuric acid. Sulfate aerosols have a large cooling effect on the global climate of about −0.4 ± 0.2 W m^{-2}.[2] While primary aerosols are released directly into the atmosphere, secondary aerosols form through the interaction of different constituent vapors present in the atmosphere.[3] New particle formation (NPF) occurs when condensable vapors nucleate to form metastable molecular clusters, which grow to produce nanometer-sized aerosol particles under certain conditions. As evidenced by the direct correlation between its concentration and nucleation rates, sulfuric acid is the main driver of NPF.[4−9] However, both field and lab measurements have shown that binary homogeneous nucleation (BHN) of sulfuric acid and water by itself cannot explain the rate of NPF observed, particularly in the lower regions of the troposphere.[10−12] Ternary bases like ammonia and amines[13−18] and organics[19−22] enhance the nucleation rate. The role of charged particles (ion-induced nucleation)[23,24] is expected to be minimal in the lower troposphere,[11,25] even though it might be important in the upper troposphere and lower stratosphere.[26]

Sulfuric acid drives the formation of secondary aerosols through BHN and ternary homogeneous nucleation (THN) involving a third (ternary) component such as ammonia, amines, or organic acids.[13,27] The sources of organic nitrogen in the atmosphere have been recently reviewed.[28,29] Ge, Wexler, and Clegg have compiled 154 atmospherically relevant amines, 32 amino acids, and urea and summarized their sources, fluxes, gas-phase reactions, and role in NPF and growth.[29−31] The main sources of methylamine (MA) are animal husbandry, fish processing, industry, automobiles, sewage treatment, biomass burning, bacteria culture, and oceans.[29] The estimated global emission of methylamine is 83 ± 26 Gg N a^{-1} (10^9 grams per annum or 10^9 grams per year) compared with 50 000 ± 30 000 Gg N a^{-1} for ammonia, 33 ± 19 Gg N a^{-1} for dimethylamine, and 169 ± 33 Gg N a^{-1} for trimethylamine.[32]

The role of amines on atmospheric nucleation has been explored computationally and experimentally. In the experimental realm, a 2011 study using the Cosmics Leaving OUtdoor Droplets (CLOUD) chamber at CERN concluded that atmospherically relevant concentrations of ammonia and amines enhanced aerosol nucleation rates by a factor of 100−1000 in the lower troposphere.[10] The work demonstrated that these bases play an important role in aerosol formation by stabilizing small particles in a process called base stabilization.

Special Issue: Kenneth D. Jordan Festschrift

Received: January 1, 2014
Revised: April 14, 2014
Published: April 15, 2014

   dx.doi.org/10.1021/jp500015t | J. Phys. Chem. A 2014, 118, 7430−7441

The effect of ternary nucleation was much more pronounced at warmer temperatures in the lower troposphere, whereas binary nucleation was more dominant at colder temperatures in the upper troposphere. In the upper troposphere and lower stratosphere, binary nucleation and ion-induced nucleation take place because of the low temperatures and the strong air exchange between troposphere and lower stratosphere.[33] A 2013 update utilizing the same CLOUD chamber further validated the idea of base stabilization by amines as an important mechanism in NPF.[11,12] The acid−amine pairs stabilize the cluster by preventing evaporation. For a H_2SO_4−DMA system, the evaporation rate is small enough that there may not be a nucleation barrier, hence a critical cluster.[12] At an atmospheric concentration of H_2SO_4 (10^6 to 10^7 cm^{-3}), dimethylamine above 3 pptv ($\sim 10^7$ cm^{-3}) was found to enhance nucleation by 1000-fold or more compared with NH_3.[12] Other experimental measurements also confirmed the enhancing effect of amines, but the extent of the enhancement was not as large. Yu et al.[18] examined the enhancing effect of five amines (methylamine, dimethylamine, trimethylamine, triethylamine, and *tert*-butylamine) in a laboratory setting and compared it with that of ammonia. Their multicomponent fast-flow nucleation reactor had H_2SO_4 concentrations of 10^6 to 10^8 cm^{-3}, amine concentrations of 0.3 to 6.0 ppbv ($\sim 10^{10}$ cm^{-3}), relative humidity (RH) of 18−80%, and a temperature of 278 K. They found that both the size and the number concentrations of the particles increased with H_2SO_4 and dimethylamine concentrations. The enhancement factor of dimethylamine on number concentrations of particles was small (<5) for particles larger than 1 nm, while it was about two orders of magnitude for particles larger than 2 nm. The enhancement factor resulting from the other amines increased with their relative basicity, thereby implying that acid−base reactions play a role in aerosol formation and growth. The basicity of these ternary species is higher than that of NH_3 (pK_b = 4.75) and increases in the order trimethylamine (pK_b = 4.22), methylamine (pK_b = 3.35), *tert*-butylamine (pK_b = 3.32), dimethylamine (pK_b = 3.27), to triethylamine (pK_b = 3.25).[18] However, other factors such as steric hindrance and the number and strength of hydrogen bonds a base molecule forms can affect its ability to enhance cluster formation. A previous study on THN with NH_3 under atmospherically relevant conditions concluded that its enhancing effect on nucleation rates was less than a factor of 10 compared with BHN[14] and that it varied depending on [H_2SO_4], [NH_3], RH, and residence times.[16] Erupe et al.[17] investigated the enhancement resulting from trimethylamine and discovered that its effect is generally moderate and comparable to that of NH_3. Despite the clear role of ternary species in aerosol formation, the concentration of H_2SO_4 (typically in the pptv range) remains the key driver even in the presence of ternary bases with much larger concentrations (in the ppbv range).[16] Zhang and coworkers have explored the role of amines in heterogeneous or multiphase aerosol chemistry.[34,35] Even though the typical concentrations of amines are two to three orders of magnitude smaller than ammonia, they could reach very high levels (hundreds of μg m^{-3} or many ppm) in areas of large industrial, sewage treatment, or animal husbandry activity. Particularly in these regions of high amine concentration, amines are expected to participate in gas-phase reactions and also in heterogeneous reactions with a condensed or aerosol phase.[35]

In the computational realm, Kurtén et al.[15] studied the effect that seven different amines (methylamine, dimethylamine, trimethylamine, ethylamine, diethylamine, triethylamine, and ethylmethylamine) have on neutral and ion-induced nucleation and compared it with that of ammonia. They calculated the binding free energy of these amines with H_2SO_4 and HSO_4^- using second-order Møller−Plesset theory (MP2) with a higher-order electron correlation correction with the second-order approximate coupled cluster singles and doubles (CC2)[36] model. They concluded that amines bind more strongly to H_2SO_4 and HSO_4^- than ammonia does because of their higher proton affinities. Even though amines are typically two to three orders of magnitude less abundant than ammonia in the atmosphere, their strong binding with H_2SO_4 and HSO_4^- makes them more potent at enhancing overall nucleation than ammonia. Loukonen et al.[37] investigated the hydration of sulfuric acid monomer and dimer bound to ammonia and dimethylamine. They concluded that dimethylamine's strong binding promotes the growth of particles in the sulfuric acid coordinate. Nadykto et al.[38] conducted a similar study on three amines (methylamine, dimethylamine, and trimethylamine) using the PW91/6-311+G(3df,3pd) density functional method. While they agreed that amines are more effective than ammonia at enhancing nucleation, they, unlike Kurtén,[15] concluded that the extent of the difference in binding energies is not enough to overcome ammonia's mass-balance advantage. Therefore, ammonia should play a larger role in NPF than amines. Because the level of theory used in studying weakly bound clusters lead to different results,[39−42] calculations that yield the most accurate estimated values for the free energy of formation of hydrogen-bonded complexes are essential for progress in understanding the beginning steps of aerosol formation.[43,44]

In this work, we focus on the effect of methylamine (MA) on sulfuric acid hydration and its implication for ternary aerosol formation. Most previous experimental and computational studies have been devoted to dimethylamine (DMA) as the amine of interest, and there is no systematic work devoted to methylamine. The estimated global emission of methylamine is 83 ± 26 Gg N a^{-1} compared with 33 ± 19 Gg N a^{-1} for dimethylamine.[29] We combine molecular dynamics (MD) simulations to sample configurations and apply high level ab initio methods to calculate the binding electronic and free energy of many stable clusters. On the basis of the Boltzmann-averaged free energies of hydration of these clusters, we calculate the equilibrium distribution of hydrates at atmospherically relevant [H_2SO_4], [CH_3NH_2], temperature, and RH. By comparing these results with the hydration of H_2SO_4 and H_2SO_4−NH_3, we assess the importance of H_2SO_4−CH_3NH_2 on aerosol formation.

2. METHODS

To find the most stable configurations of H_2SO_4−$NH_2CH_3(H_2O)_{n=0-6}$ and their thermodynamic properties, we used a scheme combining MD sampling with the ab initio RI-MP2 method. We have applied the MD/MP2 approach to water clusters, ion−water clusters, and atmospheric hydrates successfully in our previous studies.[42−53] We employed AMBER 9[54] for two-step gas-phase MD simulations using the TIP4P[55] water model along with the generalized AMBER force field (GAFF).[56] In the first step, the system was heated from 5 K to a simulation temperature T_f over a period of 1 ns. In the second step, the temperature remained at T_f for a 10 ns production run. T_f is the highest temperature at which the cluster remains intact for the whole 10 ns simulation. For H_2SO_4−$NH_2CH_3(H_2O)_n$ where n = 0−6, this simulation

dx.doi.org/10.1021/jp500015t | J. Phys. Chem. A 2014, 118, 7430−7441

Table 1. RI-MP2/CBS[a,b] Scaled Harmonic[c] Binding Energy of the Lowest Energy Isomers of H_2SO_4 with H_2O, NH_3 and CH_3NH_2

	CBS	0 K	216.65 K		273.15 K		298.15 K	
n	ΔE	ΔE_0	ΔH	ΔG	ΔH	ΔG	ΔH	ΔG
H_2SO_4–H_2O	−12.75	−10.68	−11.26	−5.15	−11.20	−3.56	−11.17	−2.87
H_2SO_4–NH_3	−16.80	−15.27	−15.67	−10.01	−15.62	−8.54	−15.59	−7.89
H_2SO_4–CH_3NH_2	−21.78	−19.90	−20.01	−13.01	−19.94	−11.41	−19.91	−10.63

[a]RI-MP2/aVDZ, RI-MP2/aVTZ//aVDZ, and RI-MP2/aVQZ//aVDZ binding energies extrapolated using eq 1. [b]All energies are in kilocalories per mole. [c]ZPVE, ΔH_{vib}(216.65 K), ΔH_{vib}(273.15 K), ΔH_{vib}(298.15 K), S_{vib}(216.65 K), S_{vib}(273.15 K), and S_{vib}(298.15 K) scaled by 0.979, 1.101, 1.083, 1.077, 1.123, 1.108, and 1.102, respectively.

temperature (T_f) was 110, 125, 125, 290, 240, 280, and 280 K for the seven simulations (n = 0–6). We sampled 300 structures from each simulation at even intervals, and these 2100 initial structures were optimized using the RI-MP2/6-31G* method. After removing duplicate structures based on energies and rotational constants, all isomers within 5 kcal mol^{-1} of the global minimum were selected for further optimization using the RI-MP2/aug-cc-pVDZ (RI-MP2/aVDZ) method. Of the resulting structures, those within 2 kcal mol^{-1} of the global minimum were reoptimized with stringent convergence criteria and harmonic vibrational frequencies were calculated at the same RI-MP2/aVDZ level of theory.

Employing Dunning's correlation consistent basis sets, aug-cc-pVNZ (abbreviated as aVNZ, where N = D, T, Q, ...)[57,58] allowed for the extrapolation of energies to the complete basis set (CBS) limit. The RI-MP2 CBS limit energies were determined using a 4–5 inverse polynomial extrapolation[59]

$$E_{CBS}^{RI-MP2} = E_N^{RI-MP2} + \frac{b}{(N+1)^4} + \frac{c}{(N+1)^5} \quad (1)$$

where E_N^{RI-MP2} is an RI-MP2/aVNZ//aVDZ energy, E_{CBS}^{RI-MP2} is the extrapolated RI-MP2/CBS energy, N is the largest angular momentum number for the aVNZ basis set (N = 2, 3, 4 for N = D, T, Q, respectively), and b and c are constants. The RI-MP2/CBS electronic energy (E_e) was combined with RI-MP2/aVDZ finite temperature thermodynamic corrections assuming ideal gas conditions with a rigid-rotor approximation for molecular rotations and a harmonic oscillator model for vibrations. Because conventional vibrational scaling factors[60−62] do not work well for hydrogen-bonded systems,[49,63,64] we derived scaling factors specifically for hydrates like the current system. To partially correct for anharmonicity, we determined scaling factors that map harmonic ZPVE and thermodynamic corrections to second-order vibrational perturbation theory (VPT2)[65] values invoking simple perturbation theory (SPT),[66] as implemented in Gaussian 09[67] for H_2SO_4 hydrates. The reason we opted to use the scaling factors from H_2SO_4 hydrates is because we were unable to get anharmonic vibrational frequencies for H_2SO_4–MA hydrates using VPT2. Because of VPT2's limitations such as numerical instabilities in the calculation of the cubic and quartic force constants as well as Fermi resonances, some of the predicted anharmonic frequencies were negative, and their corresponding infrared (IR) intensities were very large compared with their harmonic analogues. Therefore, we chose to use the scaling factors for H_2SO_4 hydrates because they resembled the H_2SO_4–MA hydrates most closely. Using three $H_2SO_4(H_2O)$ and three $H_2SO_4(H_2O)_2$ isomers as a training set, we found the multiplicative scaling factors for the ZPVE, and vibrational contributions to the enthalpy (ΔH_{vib}) and entropy (ΔS_{vib}) at three temperatures of interest in our previous work.[52] The optimal scaling factors for the ZPVE, ΔH_{vib}(216.65 K), S_{vib}(216.65 K), ΔH_{vib}(273.15 K), S_{vib}(273.15 K), ΔH_{vib}(298.15 K), and S_{vib}(298.15 K) were 0.979, 1.101, 1.123, 1.083, 1.108, 1.077, and 1.102, respectively. The unscaled harmonic thermodynamic values are included in the Supporting Information.

The binding energy of isomer i (ΔE_i) was calculated as the energy difference between the cluster and infinitely separated constituents

$$\Delta E_i = E[H_2SO_4(CH_3NH_2)(H_2O)_n]_i - E[H_2SO_4] - E[CH_3NH_2] - n^*E[H_2O] \quad (2)$$

The relative energy ($\Delta\Delta E_i$) of cluster i was calculated using the global minimum as a reference

$$\Delta\Delta E_i = E[H_2SO_4(CH_3NH_2)(H_2O)_n]_i - \min_{m=1...N}\{E[H_2SO_4(CH_3NH_2)(H_2O)_n]_m\} \quad (3)$$

The binding [$\Delta G(T)$] and relative [$\Delta\Delta G(T)$] Gibbs free energies were computed in the same fashion. Standard state conditions are 1 atm pressure and the stated temperature. All molecular graphics were generated with Chimera 1.8[68] using its default hydrogen bond definition. All RI-MP2 calculations were performed using ORCA 2.9.[69]

3. RESULTS AND DISCUSSION

3.1. Comparison of H_2SO_4–MA with H_2SO_4–NH_3 and H_2SO_4–H_2O. Table 1 compares the binding energy of H_2SO_4 with H_2O, NH_3, and CH_3NH_2.

Even though each of the three clusters (H_2SO_4–H_2O, H_2SO_4–NH_3, and H_2SO_4–CH_3NH_2) forms two hydrogen bonds, H_2SO_4–CH_3NH_2 is significantly more stable than the other two. Part of the reason for the strong H_2SO_4–CH_3NH_2 complex is the facile proton transfer leading to the formation of HSO_4^-–$CH_3NH_3^+$. In the case of H_2SO_4–NH_3, it requires the presence of at least one water molecule for proton transfer to occur, while H_2SO_4–H_2O only undergoes acid dissociation in the presence of three or more water molecules.[43,52]

The lowest energy isomers of H_2SO_4–CH_3NH_2 are shown in Figure 1. The small difference in the hydrogen bonding geometry of these isomers manifests itself in the large number of low-energy structures for the hydrated clusters.

For $H_2SO_4(CH_3NH_2)$ and $H_2SO_4(CH_3NH_2)(H_2O)$, we ran two separate MD simulations with intact (H_2SO_4–CH_3NH_2) and dissociated (HSO_4^-–$CH_3NH_3^+$) acid–base systems. However, subsequent RI-MP2 calculations on structures sampled from both sets of simulations yielded isomers with a bisulfate-methylammonium (HSO_4^-–$CH_3NH_3^+$) salt as the

dx.doi.org/10.1021/jp500015t | J. Phys. Chem. A 2014, 118, 7430–7441

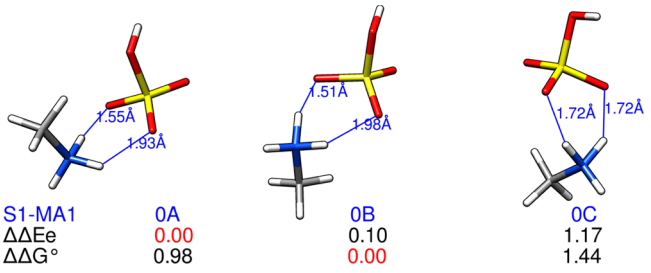

Figure 1. RI-MP2/CBS low-energy isomers of $H_2SO_4(CH_3NH_2)$. The relative scaled harmonic Gibbs free energy is at a standard state of 298.15 K and 1 atm.

lowest energy isomers. The most stable isomer with H_2SO_4–CH_3NH_2 as an undissociated acid–base system was at least 7 kcal mol^{-1} higher in electronic energy than the global minimum for $H_2SO_4(CH_3NH_2)$. Therefore, acid–base reactions between H_2SO_4 and CH_3NH_2 occur even in the gas phase in the absence of water. Water molecules typically play an important role in proton-transfer reactions through aggregation-induced acid dissociation.[70−73] The acid dissociation of strong monoprotic acids requires three to five water molecules.[74] The relative stability of the neutral and dissociated species depends on the proton transfer energy, Coulombic attraction, and hydrogen-bond stabilization.[74] For $H_2SO_4(H_2O)_{n=1-6}$, the clusters containing the deprotonated H_2SO_4 become the global minima in terms of E_e and G(298.15 K) when $n \geq 4$ and $n = 6$, respectively.[43,52] The three isomers of $H_2SO_4(CH_3NH_2)$ shown in Figure 1 all have two hydrogen bonds (HBs) each. In the case of isomers 0A and 0B, the two HBs differ significantly in strength and geometry: the HB distances for the stronger and weaker HBs are 1.51 to 1.55 Å and 1.93 to 1.98 Å, respectively. Such differences in HB strength and geometry are not unusual. For example, the lowest energy isomers of $H_2SO_4(H_2O)$ have a primary (strong) and secondary (weak) HB.[52] The strength of the primary and secondary HBs was estimated to be 8 to 9 and 3 to 4 kcal mol^{-1}, respectively.[75] $HSO_4^-(H_2O)$ also exhibits a similar pair of strong and weak HBs.[44] Isomers 0A and 0B are nearly isoenergetic, but 0B is more stable once ZPVE and entropic corrections are included. Isomer 0C has two HBs of medium strength, and their HB length is 1.72 Å. In all three isomers, the amine group is donating both HBs and the methyl group is unencumbered. Therefore, the methyl group should be able to undergo hindered or free rotations at most temperatures. The standard binding enthalpy [H^0(298 K)] and Gibbs free energy [G^0(298 K)] of structure 0B compare well with that of the G^0(298 K) global minimum from Kurtén et al.'s[15] RI-CC2/aug-cc-pV(T+d)Z//RI-MP2/aug-cc-pV(D+d)Z and Nadykto et al.'s[38] PW91/6-311+G(3df,3pd) calculations. This comparison is presented in Table 2. The small differences can be attributed to the levels of theory and basis sets used as well as vibrational anharmonicity corrections.

3.2. Structure and Stability of Hydrates. The structures of all hydrates whose relative RI-MP2/CBS electronic energy ($\Delta\Delta E_e$) is within 2 kcal mol^{-1} of the putative global minimum isomer are reported here. The isomers of $H_2SO_4(CH_3NH_2)$-$(H_2O)_n$ are ordered in increasing relative energy ($\Delta\Delta E_e$) and labeled as nA, nB, nC, and so on. Their relative electronic ($\Delta\Delta E_e$) and standard Gibbs free energy ($\Delta\Delta G^0$) at 298.15 K and 1 atm are also given to assess their relative stability. The binding thermodynamics (Tables S1–S7 in the Supporting Information) and Cartesian coordinates (Tables S17–S23 in the Supporting Information) of each isomer are reported in the Supporting Information. The interested reader can find the binding thermodynamics based on unscaled harmonic values in Tables S10–S16 in the Supporting Information. The 20 isomers of $H_2SO_4(CH_3NH_2)(H_2O)$ whose $\Delta\Delta E_e$ is within 2 kcal mol^{-1} of the global minimum (1A) are shown in Figure 2. As expected, there is a proton transfer from the acid to the base.

The added water forms an HB to HSO_4^- as a donor (D) and another with $CH_3NH_3^+$ as an acceptor (A). With the exception of isomer 1H, each isomer has three HBs connecting the three constituents. The $CH_3NH_3^+$ moiety donates strong HBs to HSO_4^- and H_2O with HB distances of 1.5 to 1.6 Å and ∼1.7 to 1.8 Å, respectively. Even though all isomers have similar hydrogen-bonding properties, the presence of the unencumbered methyl group of methylamine and its orientation relative to the rest of the cluster leads to many nearly isoenergetic minima. The electronic energy global minimum (1A) is energetically favorable at all temperatures up to 298.15 K, but entropic considerations make isomer 1J the most stable structure past 216.65. Nadykto et al.'s[38] PW91/6-311+G(3df,3pd) global minimum structure does not correspond to any of the low-energy isomers in our work. Nevertheless, the ΔH^0(298 K) and ΔG^0(298 K) values agree within 1 kcal mol^{-1}, as shown in Table 2.

As shown in Figure 3, the eight lowest energy isomers of $H_2SO_4(CH_3NH_2)(H_2O)_2$ all have five HBs, each with HSO_4^- accepting two or three HBs and $CH_3NH_3^+$ donating two or three HBs. The two water molecules are involved as single donor–acceptors (DAs) with the exception of isomer 2G, where one water is a single acceptor-double donor (DDA). In general, the waters bridge HSO_4^- with $CH_3NH_3^+$ such that the average distance between the two is longer than it was in the case of $H_2SO_4(CH_3NH_2)(H_2O)_{n=0-1}$. Once again, the global minimum structure reported by Nadykto et al.'s[38] PW91/6-311+G(3df,3pd) work does not correspond to any of the low energy isomers in our work, but the ΔH^0(298 K) and ΔG^0(298 K) values agree within 1 kcal mol^{-1}, as shown in Table 2.

Table 2. Comparison of the Standard Enthalpy and Gibbs Free Energy of $H_2SO_4(CH_3NH_2)(H_2O)_n$, where n = 0–2 Previous Literature[a]

	current[b]		Nadykto et al.[c]		Kurtén et al.[d]	
	ΔH^0	ΔG^0	ΔH^0	ΔG^0	ΔH^0	ΔG^0
$H_2SO_4 + CH_3NH_2$	−19.91	−11.61	−20.40	−11.03	−20.87	−9.95
$H_2SO_4(CH_3NH_2) + H_2O$	−12.55	−3.53	−13.02	−3.33		
$H_2SO_4(CH_3NH_2)H_2O + H_2O$	−13.10	−3.95	−13.85	−3.52		

[a]Clusters correspond to the G^0(298.15 K) global minima. [b]RI-MP2/CBS with anharmonicity corrections to the ZPVE and vibrational entropy and enthalpy. The G^0(298.15 K) global minima in the current work are 0B, 1J, and 2A. [c]Ref 38. PW91/6-311+G(3df,3pd) without anharmonicity corrections [d]Ref 15. RI-CC2/aug-cc-pV(T+d)Z//RI-MP2/aug-cc-pV(D+d)Z without anharmonicity corrections

dx.doi.org/10.1021/jp500015t | J. Phys. Chem. A 2014, 118, 7430−7441

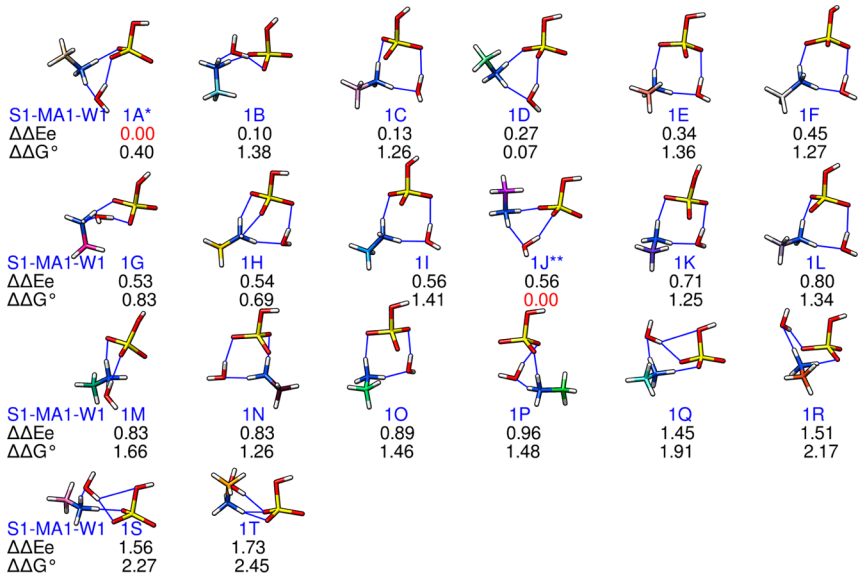

Figure 2. RI-MP2/CBS low-energy isomers of $H_2SO_4(CH_3NH_2)H_2O$. The relative scaled harmonic Gibbs free energy is at a standard state of 298.15 K and 1 atm. The * and ** indicate the E_e and G^0 (298 K) global minima.

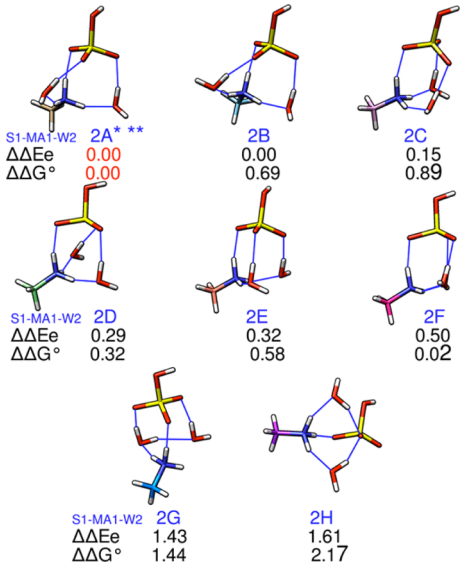

Figure 3. RI-MP2/CBS low-energy isomers of $H_2SO_4(CH_3NH_2)(H_2O)_2$. The relative scaled harmonic Gibbs free energy is at a standard state of 298.15 K and 1 atm. The * and ** indicate the E_e and G^0 (298 K) global minima.

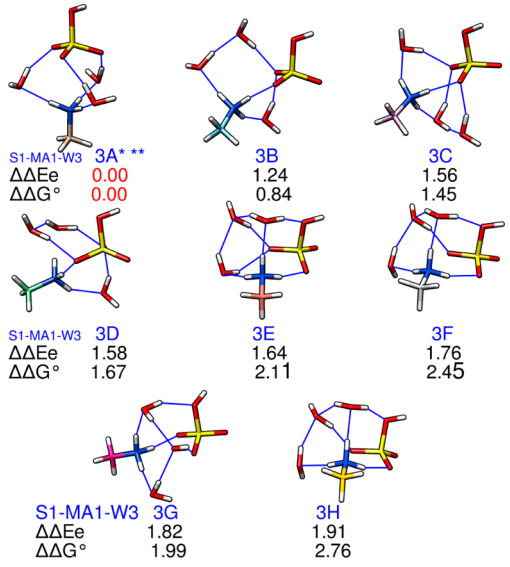

Figure 4. RI-MP2/CBS low-energy isomers of $H_2SO_4(CH_3NH_2)(H_2O)_3$. The relative scaled harmonic Gibbs free energy is at a standard state of 298.15 K and 1 atm. The * and ** indicate the E_e and G^0 (298 K) global minima.

The $H_2SO_4(CH_3NH_2)(H_2O)_3$ isomers in Figure 4 have six to eight HBs, and the most stable isomer (3A) has three bridging waters between the HSO_4^- and $CH_3NH_3^+$ ions.

Because of differences in the strength of the HBs, some isomers that have seven or eight HBs are less stable than 3A that has only six HBs. $H_2SO_4(CH_3NH_2)(H_2O)_4$ has 20 isomers with 7−9 HBs each, as displayed in Figure 5. Although 4A is the most stable isomer based on its E_e, inclusion of ZPVE and finite temperature corrections establishes 4B as the global minimum. Most of the low-energy isomers have HSO_4^- accepting three HBs, but the higher energy ones such as 4H have HSO_4^- accepting a fourth HB. Isomers like 4O and 4S have the hydroxyl group of HSO_4^- donating a HB to a water molecule. As shown in Figure 6, adding a fifth water leads to further separation of the HSO_4^- and $CH_3NH_3^+$ species, with the waters playing a bridging role.

Unlike $H_2SO_4(CH_3NH_2)(H_2O)_4$, the hydroxyl group of HSO_4^- donates an HB to a water molecule only in isomer 5H. The isomers have 10 to 11 HBs each with the exception of 5H, which has 12 HBs but remains entropically unfavorable ($\Delta\Delta G^0$ = 3.98 kcal mol^{-1}). $H_2SO_4(CH_3NH_2)(H_2O)_5$ has unusual stability based on its electronic energy, as demonstrated by the dip in ΔE_e in Figure 8. The reason for this stability is not clear, although a similar pattern has been seen for $HSO_4^-(H_2O)_5$.[44] The $HSO_4^-(H_2O)_5$ cluster has unusual stability according to our RI-MP2/CBS calculations and an experimental quadruple time-of-flight mass spectroscopic (QTOF-MS) study by Zatula et al.,[76] which showed increased abundance of the $HSO_4^-(H_2O)_5$ cluster compared with $HSO_4^-(H_2O)_4$ and

dx.doi.org/10.1021/jp500015t | J. Phys. Chem. A 2014, 118, 7430−7441

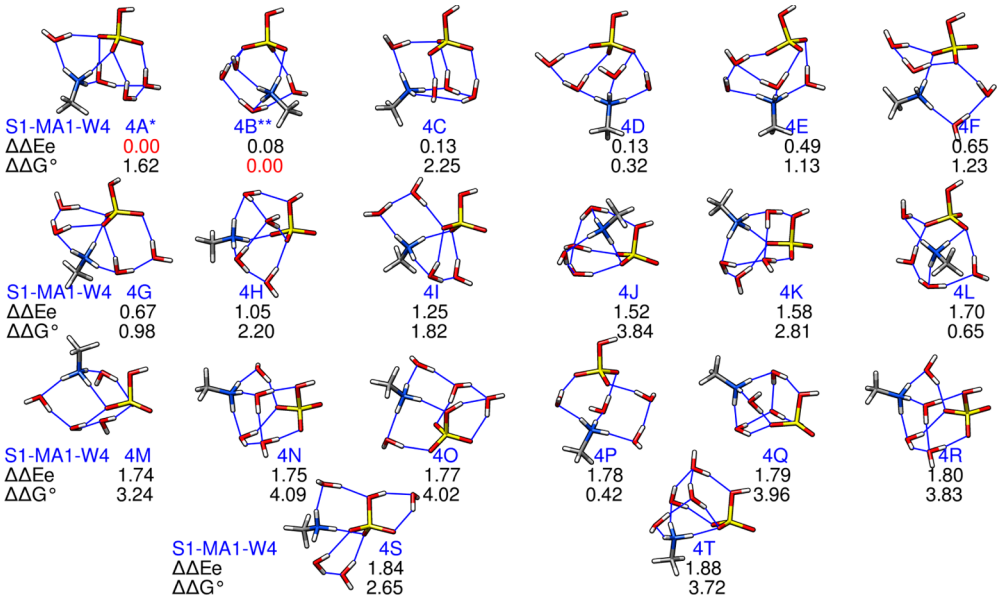

Figure 5. RI-MP2/CBS low-energy isomers of $H_2SO_4(CH_3NH_2)(H_2O)_4$. The relative scaled harmonic Gibbs free energy is at a standard state of 298.15 K and 1 atm. The * and ** indicate the E_e and G^0 (298 K) global minima.

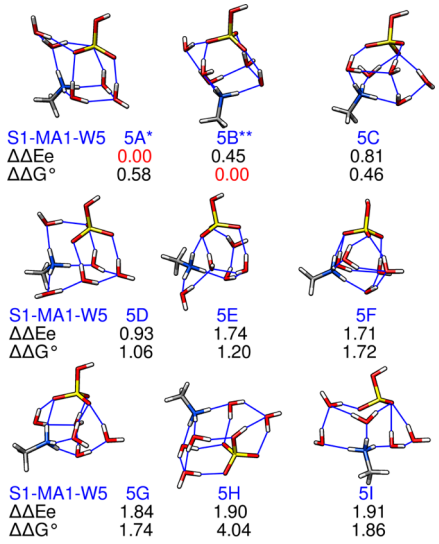

Figure 6. RI-MP2/CBS low-energy isomers of $H_2SO_4(CH_3NH_2)(H_2O)_5$. The relative scaled harmonic Gibbs free energy is at a standard state of 298.15 K and 1 atm. The * and ** indicate the E_e and G^0 (298 K) global minima.

$HSO_4^-(H_2O)_6$. Lastly, the 17 isomers of $H_2SO_4(CH_3NH_2)(H_2O)_6$ isomers shown in Figure 7 have 12 to 13 HBs each. In some isomers such as 6B, HSO_4^- is fully hydrogen bonded by accepting four HBs and donating one HB, while it only accepts three HBs in others like 6A. The competition between the two hydrogen-bonding patterns is evident from the comparable number of isomers exhibiting these two motifs. Structure 6A is the E_e global minimum, while entropic corrections stabilize 6C with increasing temperature. The bridging role of the water molecules continues just as it did for smaller clusters; the majority of the isomers do not have a direct HB between the HSO_4^- and $CH_3NH_3^+$ ions.

3.3. Thermodynamics of Hydration. The enthalpy (ΔH) and Gibbs free energy (ΔG) of each isomer have been Boltzmann-averaged at three atmospherically relevant temperatures: 216.15 K, the average temperature of the tropopause; 273.15 K; and room temperature (298.15 K). The change in electronic energy (ΔE_e), zero-point vibrational energy corrected energy (ΔE_0), $\Delta H^0(T)$, and $\Delta G^0(T)$ upon the stepwise addition of water is shown in Figure 8.

The Figure illustrates that the initial formation of an H_2SO_4–CH_3NH_2 complex (n = 0) is highly favorable; however, the subsequent addition of water molecules to an existing cluster is less thermodynamically favorable. The enthalpy change associated with the stepwise addition of waters is highly exothermic with $\Delta H^0(T)$ values of −20 to −8 kcal mol^{-1}. However, entropic effects limit the stepwise addition of water, particularly for clusters containing more than two water molecules at $T \geq 273$ K.

The n = 0 values refer to the reaction of H_2SO_4 and CH_3NH_2 to form $HSO_4^-CH_3NH_3^+$, which is very favorable thermodynamically. The stepwise addition of the first and second water is also largely favorable, but adding a third water is less favorable, as demonstrated in the spike at n = 3 in Figure 8. Adding a fourth and fifth water is more favorable in terms of both ΔH and ΔG, even though the trend clearly shows that the extent of stabilization is decreasing with increasing number of waters. The standard Gibbs free energy of stepwise addition (ΔG^0) remains negative for n = 0–6 up to T = 273.15 K, while it becomes positive for n = 3 and 6 at T = 298.15 K. One can safely assume that adding water molecules past n = 6 will be unfavorable particularly at higher temperatures.

The comparison of the hydration thermodynamics of $H_2SO_4(CH_3NH_2)$ and H_2SO_4 in Figure 9 provides useful insight about the role of methylamine in these hydrates. The stepwise hydration energies for both sets of clusters are directly comparable because they are calculated using RI-MP2/CBS electronic energies and scaled harmonic thermodynamic values. The main difference in the hydration thermodynamics of $H_2SO_4(CH_3NH_2)$ and H_2SO_4 is for n = 1 to 2, where the presence of methylamine clearly stabilizes the cluster and promotes the addition of the first two waters. For $n \geq 3$, the addition of water molecules to existing clusters is no more favorable for methylamine-containing clusters than it is for

dx.doi.org/10.1021/jp500015t | J. Phys. Chem. A 2014, 118, 7430–7441

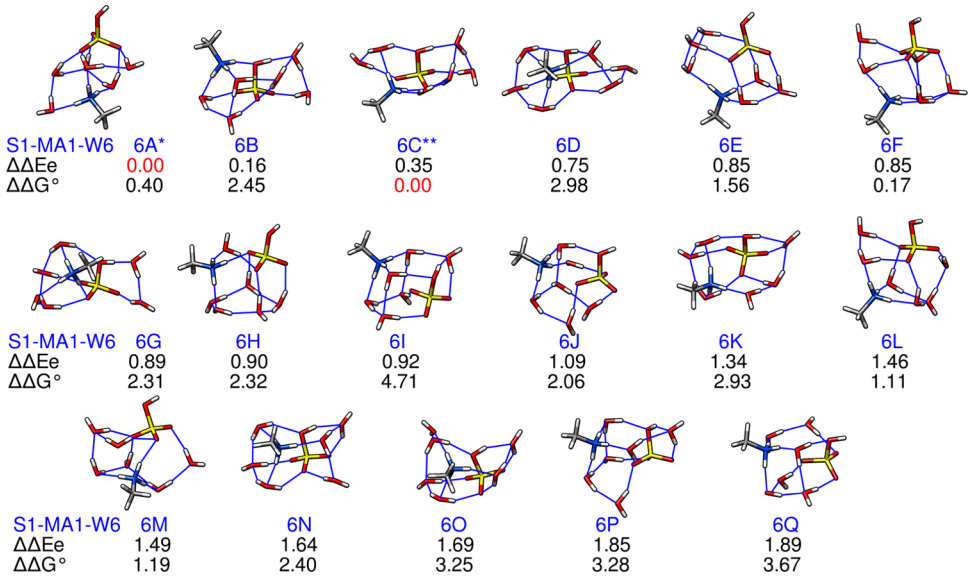

Figure 7. RI-MP2/CBS low-energy isomers of $H_2SO_4(CH_3NH_2)(H_2O)_6$. The relative scaled harmonic Gibbs free energy is at a standard state of 298.15 K and 1 atm. The * and ** indicate the E_e and G^0 (298 K) global minima.

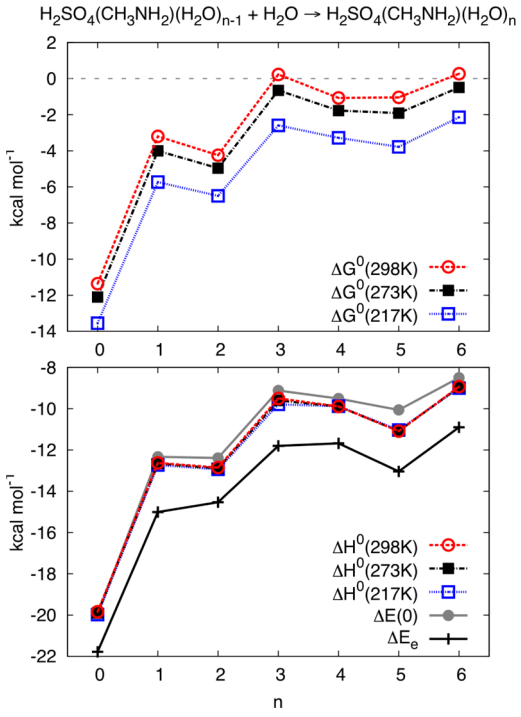

Figure 8. RI-MP2/CBS scaled harmonic Boltzmann-averaged thermodynamics of stepwise hydration of H_2SO_4–CH_3NH_2, $H_2SO_4(CH_3NH_2)(H_2O)_{n-1} + H_2O \rightarrow H_2SO_4(CH_3NH_2)(H_2O)_n$. n = 0 corresponds to the binding energy of H_2SO_4 and CH_3NH_2 in the absence of water. See Table 3 for numerical values.

$H_2SO_4(H_2O)_n$ clusters. This observation is understandable considering that HSO_4^- and $CH_3NH_3^+$ do not remain hydrogen bonded as more waters are added. Instead, the water molecules separate the acid and base and form bridging HBs between them. The presence of a methyl group sterically limits methylamine's involvement in hydrogen bonding with water molecules and H_2SO_4. Therefore, the ability of methylamine to promote the hydration of sulfuric acid diminishes with an increasing number of water molecules.

The use of scaling factors developed for H_2SO_4 hydrates to H_2SO_4–MA hydrates would slightly overestimate the effect of anharmonicity for the smallest clusters. In fact, we see that the anharmonicity correction to the stepwise ΔG(298.15 K) is −0.86 kcal/mol for H_2SO_4–MA compared with −0.32, −0.34, −0.28, −0.39, −0.27, and −0.35 for H_2SO_4–MA$(H_2O)_{n=1-6}$, respectively. However, this scaling approach is still significantly better than the alternatives such as excluding anharmonicity corrections altogether or applying scaling factors developed for non-hydrogen-bonded systems.

3.4. Atmospheric Abundance and Implications for Aerosol Formation. On the basis of the scaled harmonic stepwise Gibbs free energies of hydration given at the bottom of Table 3, we calculated the equilibrium hydrate populations for a given concentration of H_2SO_4, CH_3NH_2, and H_2O at a standard state of 1 atm pressure and temperature (T). The temperature and relative humidity (RH) range studied here are representative of what is observed in the troposphere: T = 216.65, 273.15, 298.15 K and RH = 20, 50, 80, and 100%.[3] The number concentration of water vapor at saturation (RH = 100%) corresponds to 9.89×10^{14} cm^{-3}, 1.62×10^{17} cm^{-3}, and 7.70×10^{17} cm^{-3} at the three temperatures.[3] The typical concentration of H_2SO_4 in the lower troposphere is 10^6 to 10^7 cm^{-3}, and it decreases to 10^5 cm^{-3} at the tropopause.[26,77] Experimental measurements of the gas-phase concentration of MA are rare, and the latest chemical ionization mass spectrometer (CIMS) measurements report that it should be 10^7 cm^{-3} or lower.[78]

The equilibrium hydrate populations under atmospherically relevant conditions are determined by solving the mass-balance equations. The distribution at of H_2SO_4 hydrates plotted in Figure 10a indicates that the most prevalent species in this closed system are unhydrated (n = 0) H_2SO_4 and monohydrate (n = 1), even though the dihydrate (n = 2) and trihydrate (n = 3) are present in appreciable amounts at larger RH values.[52] Figure 10b shows that the dihydrate, $H_2SO_4(MA)(H_2O)_2$ is by far the most abundant species among the H_2SO_4–MA clusters. As Figure 8 illustrates, the dihydrate, $H_2SO_4(MA)(H_2O)_2$, is more stable than the smaller monohydrate, $H_2SO_4(MA)H_2O$, and larger trihydrate, $H_2SO_4(MA)(H_2O)_3$, over the temper-

dx.doi.org/10.1021/jp500015t | J. Phys. Chem. A 2014, 118, 7430−7441

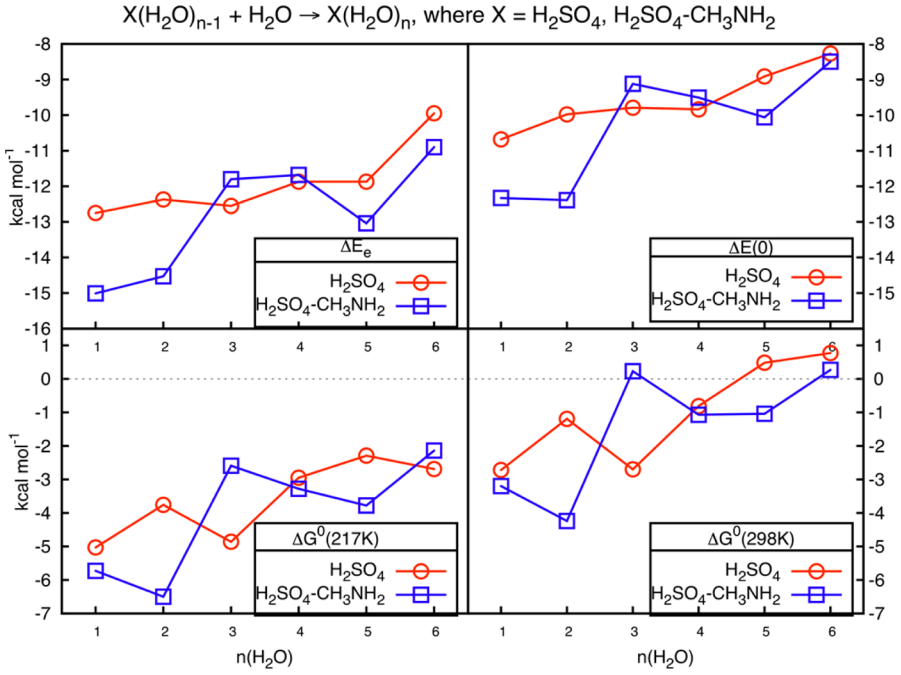

Figure 9. Comparison of the RI-MP2/CBS scaled harmonic stepwise hydration thermodynamics of H_2SO_4 and H_2SO_4–NH_2CH_3. Even though the first (n = 1) and second (n = 2) waters are more strongly bound to H_2SO_4–NH_2CH_3 than H_2SO_4, additional water molecules are bound equivalently to both.

Table 3. RI-MP2/CBS[a,b] Scaled Harmonic[c] Boltzmann-Averaged Energy Change upon the Stepwise Addition of Water to $H_2SO_4(H_2O)_{n-1}$ and $H_2SO_4(CH_3NH_2)(H_2O)_{n-1}$ at a Standard State of 1 atm and the Given Temperature

	CBS	0 K	216.65 K		273.15 K		298.15 K	
n	ΔE	ΔE_0	ΔH	ΔG	ΔH	ΔG	ΔH	ΔG
			$H_2SO_4(H_2O)_{n-1} + H_2O \rightarrow H_2SO_4(H_2O)_n$					
1	−12.75	−10.68	−11.16	−5.03	−11.07	−3.42	−11.02	−2.72
2	−12.37	−9.98	−10.53	−3.76	−10.49	−1.96	−10.45	−1.19
3	−12.55	−9.79	−10.64	−4.86	−10.69	−3.39	−10.71	−2.70
4	**−11.87**	−9.84	−10.57	−2.95	−10.72	−1.59	−10.71	−0.81
5	**−11.87**	−8.91	−9.95	−2.29	−9.78	−0.22	−9.71	0.48
6	−9.95	−8.27	−8.89	−2.69	−8.90	−0.24	−8.90	0.77
			$H_2SO_4(CH_3NH_2)(H_2O)_{n-1} + H_2O \rightarrow H_2SO_4(CH_3NH_2)(H_2O)_n$					
-	−21.78	−19.97	−19.98	−13.55	−19.89	−12.10	−19.84	−11.36
1	−15.01	−12.33	−12.73	−5.73	−12.66	−4.00	−12.63	−3.20
2	−14.53	−12.39	−12.94	−6.50	−12.89	−4.96	−12.85	−4.24
3	−11.80	−9.12	−9.79	−2.59	−9.60	−0.65	−9.50	0.23
4	−11.68	−9.51	−9.88	−3.28	−9.89	−1.77	−9.89	−1.07
5	−13.04	−10.06	−11.03	−3.78	−11.08	−1.91	−11.09	−1.04
6	−10.90	−8.50	−9.00	−2.14	−8.96	−0.49	−8.93	0.27

[a]RI-MP2/aVDZ, RI-MP2/aVTZ//aVDZ, and RI-MP2/aVQZ//aVDZ binding energies extrapolated using eq 1. [b]All energies are in kilocalories per mole. [c]ZPVE, ΔH_{vib}(216.65 K), ΔH_{vib}(273.15 K), ΔH_{vib}(298.15 K), S_{vib}(216.65 K), S_{vib}(273.15 K), and S_{vib}(298.15 K) scaled by 0.979, 1.101, 1.083, 1.077, 1.123, 1.108, and 1.102, respectively.

ature range considered here. Therefore, it is expected that the population of the dihydrate is large. At lower RH values and higher temperatures, more of the unhydrated H_2SO_4 monomer is predicted to be present, but the unhydrated H_2SO_4–MA remains small relative to H_2SO_4–$MA(H_2O)_2$. Our current study suggests that the presence of methylamine favors the formation of dihydrates compared with the H_2SO_4–H_2O cluster. Loukonen et al.[37] investigated the hydration of H_2SO_4–DMA and found the monohydrate, H_2SO_4–$DMA(H_2O)$ to be the most prevalent species. The average number of water molecules around H_2SO_4 and H_2SO_4–MA, $<n_{H_2O}>$, is shown in Table 4. Not surprisingly, $<n_{H_2O}>$ for H_2SO_4–MA is around 2 at all temperatures and RHs because the dihydrate is the most dominant species. $<n_{H_2O}>$ for H_2SO_4 ranges from 0.41 at T = 298.15 K and RH = 20% to 1.67 at T = 216.65 K and RH = 100%. Therefore, the hydration of H_2SO_4–MA shows a very small dependence on temperature and RH.

While the focus here has been on the effect of MA in enhancing the hydration of H_2SO_4, the role of water in stabilizing small clusters becomes less important in the presence of an amine like MA that binds strongly to sulfuric acid. Both water and MA compete to bind to sulfuric acid, and

dx.doi.org/10.1021/jp500015t | J. Phys. Chem. A 2014, 118, 7430−7441

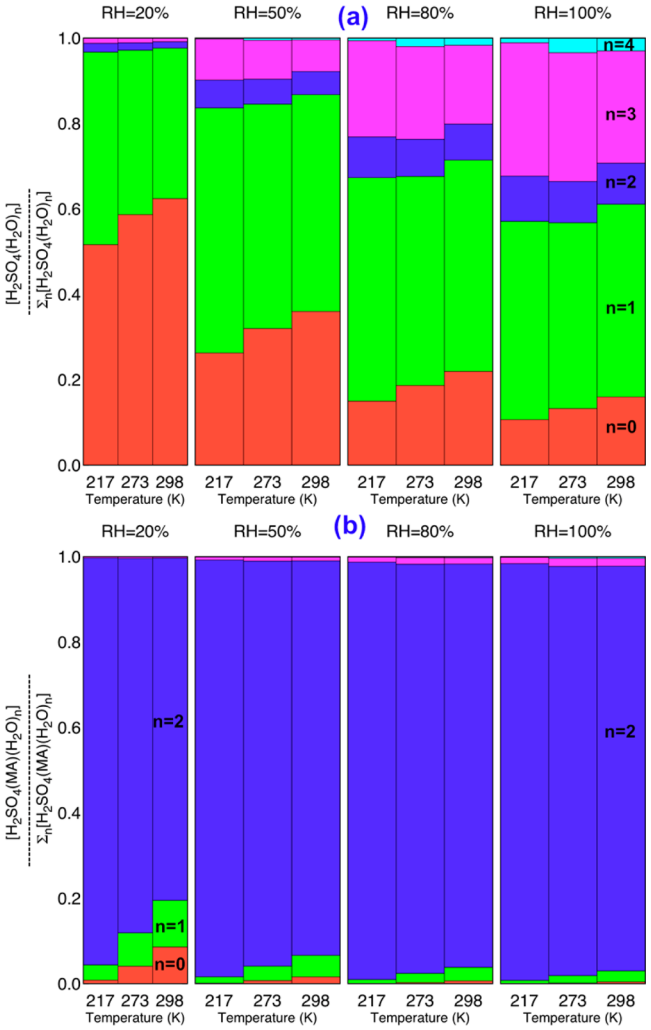

Figure 10. Equilibrium distribution of H_2SO_4 (a) and H_2SO_4–MA (b) hydrates as a function of temperature and relative humidity (RH) based on scaled harmonic Gibbs free energies of hydration. The saturation (100% RH) vapor pressure of $[H_2O]$ is assumed to be 9.9×10^{14}, 1.6×10^{17}, and 7.7×10^{17} cm^{-3} at T = 216.65, 273.15, and 298.15 K, respectively. The population of n = 5 and 6 clusters is too small to appear in the Figure.

Table 4. Average Number of Water Molecules, $<n_{H_2O}>$, around H_2SO_4 and H_2SO_4–MA at Various Temperatures and Relative Humidity (RH) Values[a]

		RH			
temperature (K)	system	20%	50%	80%	100%
216.65	H_2SO_4	0.53	1.00	1.40	1.67
	H_2SO_4–MA	1.94	2.00	2.01	2.02
273.15	H_2SO_4	0.45	0.94	1.39	1.67
	H_2SO_4–MA	1.84	1.96	1.99	2.01
298.15	H_2SO_4	0.41	0.85	1.29	1.55
	H_2SO_4–MA	1.72	1.93	1.97	1.99

[a]See Figure 10 for details.

each has a stabilizing effect; water stabilizes H_2SO_4–MA clusters just as MA stabilizes H_2SO_4–H_2O clusters. The enhancement of aerosol formation in the presence of amines has been demonstrated in recent experimental studies.[10−12,14,16−18] Experiments at CERN's CLOUD chamber have suggested that the mechanism to enable and enhance aerosol formation is through base-stabilization. In this mechanism, sulfuric acid and amines are present in a 1:1 ratio in the early steps of aerosol formation.[10−12] Our finding suggests that methylamine promotes the hydration of H_2SO_4 while also stabilizing small clusters. To fully investigate this base stabilization mechanism, one would need to examine the thermodynamics with multiple sulfuric acids and amines present together – $(H_2SO_4)_p(CH_3NH_2)_q$, where $p > 1$ and $q > 1$. Recent works investigating the thermodynamics of cluster formation not only along the water coordinate (hydration) but also along the sulfuric acid and amine coordinates provide more reliable insight into the role of amines.[79−82] In addition, examining the growth and evaporation kinetics of clusters is important.[83]

4. CONCLUSIONS

The hydration of a system of sulfuric acid (H_2SO_4) and methylamine (NH_2CH_3) with up to six waters was investigated to assess the role of ternary species on aerosol formation. By combining MD sampling with high-level ab initio calculations, the thermodynamics of forming $H_2SO_4(NH_2CH_3)(H_2O)_n$ clusters was determined. As a strong acid–base system, H_2SO_4–NH_2CH_3 quickly forms a tightly bound HSO_4^-–$NH_3CH_3^+$ complex, on which water condenses more readily than it would on H_2SO_4 alone. Even though adding one to two water molecules to an H_2SO_4–NH_2CH_3 cluster is more favorable than for H_2SO_4 alone, there is no systematic difference for $n \geq 3$. This is because additional waters bridge the acid–base cluster, separating the acid and base and moving the charged ions further apart. The assessment of the base-stabilization mechanism that has been proposed to explain the enhancing effect of amines requires an investigation of larger systems containing sulfuric acid and amines in a 1:1 ratio.

■ ASSOCIATED CONTENT

Supporting Information

The RI-MP2/CBS electronic energy, harmonic and scaled harmonic binding enthalpies, and Gibbs free energies at 0, 216.65, 273.15, and 298.15 K and RI-MP2/aVDZ optimized coordinates of all $H_2SO_4(CH_3NH_2)(H_2O)_n$ clusters reported here. This material is available free of charge via the Internet at http://pubs.acs.org.

■ AUTHOR INFORMATION

Corresponding Author

*E-mail: george.shields@bucknell.edu.

Notes

The authors declare no competing financial interest.

■ ACKNOWLEDGMENTS

We thank the reviewers for their helpful comments. Acknowledgment is made to the NSF and Bucknell University for their support of this work. This project was partially supported by NSF grants CHE-0848827 and CHE-1213521 and by NSF grants CHE-0116435, CHE-0521063, CHE-0849677, and CHE-1229354 as part of the MERCURY high-performance computer consortium (http://www.mercuryconsortium.org). This research used the National Science Foundation XSEDE resources provided by the Texas Advanced Computing Center (TACC) under grant numbers TG-CHE090095 and TG-CHE120025. This research also used resources of the National

Energy Research Scientific Computing Center, which is supported by the Office of Science of the U.S. Department of Energy under Contract No. DE-AC02-05CH11231.

REFERENCES

(1) Foster, P.; Ramaswamy, V. Changes in Atmospheric Constituents and Radiative Forcing. In *Climate Change 2007 The Scientific Basis*; Solomon, S., Qin, D., Manning, M., Chen, Z., Marquis, M., Averyt, K. B., Tignor, M., Miller, H. L., Eds.; Cambridge University Press: Cambridge, U.K., 2007; pp 131−217.

(2) Solomon, S.; Qin, D.; Manning, M. *Climate Change 2007: The Physical Science Basis*; Cambridge University Press: Cambridge, U.K., 2007.

(3) Seinfeld, J. H.; Pandis, S. N. *Atmospheric Chemistry and Physics: From Air Pollution to Climate Change*, 2nd ed.; John Wiley & Sons, Inc.: New York, 2006.

(4) Kulmala, M.; Vehkamäki, H.; Petäjä, T.; Dal Maso, M.; Lauri, A.; Kerminen, V. M.; Birmili, W.; McMurry, P. H. Formation and growth rates of ultrafine atmospheric particles: a review of observations. *J. Aerosol Sci.* **2004**, *35*, 143−176.

(5) Kuang, C.; McMurry, P. H.; McCormick, A. V.; Eisele, F. L. Dependence of nucleation rates on sulfuric acid vapor concentration in diverse atmospheric locations. *J. Geophys. Res.* **2008**, *113*, D10209.

(6) Kerminen, V. M.; Petäjä, T.; Manninen, H. E.; Paasonen, P.; Nieminen, T.; Sipilä, M.; Junninen, H.; Ehn, M.; Gagné, S.; Laakso, L.; et al. Atmospheric nucleation: highlights of the EUCAARI project and future directions. *Atmos. Chem. Phys. Discuss.* **2010**, *10*, 16497−16549.

(7) Sipilä, M.; Berndt, T.; Petäjä, T.; Brus, D.; Vanhanen, J.; Stratmann, F.; Patokoski, J.; Mauldin, R. L.; Hyvarinen, A. P.; Lihavainen, H.; et al. The Role of Sulfuric Acid in Atmospheric Nucleation. *Science* **2010**, *327*, 1243−1246.

(8) Bzdek, B. R.; Zordan, C. A.; Luther, G. W., III; Johnston, M. V. Nanoparticle Chemical Composition During New Particle Formation. *Aerosol Sci. Technol.* **2011**, *45*, 1041−1048.

(9) Bzdek, B. R.; Johnston, M. V. New Particle Formation and Growth in the Troposphere+. *Anal. Chem.* **2010**, *82*, 7871−7878.

(10) Kirkby, J.; Curtius, J.; Almeida, J.; Dunne, E.; Duplissy, J.; Ehrhart, S.; Franchin, A.; Gagne, S.; Ickes, L.; Kurten, A.; et al. Role of sulphuric acid, ammonia and galactic cosmic rays in atmospheric aerosol nucleation. *Nature* **2011**, *476*, 429−433.

(11) Kulmala, M.; Kontkanen, J.; Junninen, H.; Lehtipalo, K.; Manninen, H. E.; Nieminen, T.; Petäjä, T.; Sipilä, M.; Schobesberger, S.; Rantala, P.; et al. Direct Observations of Atmospheric Aerosol Nucleation. *Science* **2013**, *339*, 943−946.

(12) Almeida, J.; Schobesberger, S.; Kurten, A.; Ortega, I. K.; Kupiainen-Maatta, O.; Praplan, A. P.; Adamov, A.; Amorim, A.; Bianchi, F.; Breitenlechner, M.; et al. Molecular understanding of sulphuric acid-amine particle nucleation in the atmosphere. *Nature* **2013**, *502*, 359−363.

(13) Zhang, R.; Khalizov, A.; Wang, L.; Hu, M.; Xu, W. Nucleation and Growth of Nanoparticles in the Atmosphere. *Chem. Rev.* **2012**, *112*, 1957−2011.

(14) Benson, D. R.; Young, L. H.; Kameel, F. R.; Lee, S. H. Laboratory-measured nucleation rates of sulfuric acid and water binary homogeneous nucleation from the SO2 + OH reaction. *Geophys. Res. Lett.* **2008**, *35*, L11801.

(15) Kurtén, T.; Loukonen, V.; Vehkamäki, H.; Kulmala, M. Amines are likely to enhance neutral and ion-induced sulfuric acid-water nucleation in the atmosphere more effectively than ammonia. *Atmos. Chem. Phys.* **2008**, *8*, 4095−4103.

(16) Benson, D. R.; Yu, J. H.; Markovich, A.; Lee, S. H. Ternary homogeneous nucleation of H_2SO_4, NH_3, and H_2O under conditions relevant to the lower troposphere. *Atmos. Chem. Phys.* **2011**, *11*, 4755−4766.

(17) Erupe, M. E.; Viggiano, A. A.; Lee, S. H. The effect of trimethylamine on atmospheric nucleation involving H_2SO_4. *Atmos. Chem. Phys.* **2011**, *11*, 4767−4775.

(18) Yu, H.; McGraw, R.; Lee, S.-H. Effects of amines on formation of sub-3 nm particles and their subsequent growth. *Geophys. Res. Lett.* **2012**, *39*L02807.

(19) Zhang, R.; Suh, I.; Zhao, J.; Zhang, D.; Fortner, E. C.; Tie, X.; Molina, L. T.; Molina, M. J. Atmospheric New Particle Formation Enhanced by Organic Acids. *Science* **2004**, *304*, 1487−1490.

(20) Metzger, A.; Verheggen, B.; Dommen, J.; Duplissy, J.; Prevot, A. S. H.; Weingartner, E.; Riipinen, I.; Kulmala, M.; Spracklen, D. V.; Carslaw, K. S.; et al. Evidence for the role of organics in aerosol particle formation under atmospheric conditions. *Proc. Natl. Acad. Sci.* **2010**, *107*, 6646−6651.

(21) Wang, L.; Khalizov, A. F.; Zheng, J.; Xu, W.; Ma, Y.; Lal, V.; Zhang, R. Atmospheric nanoparticles formed from heterogeneous reactions of organics. *Nat. Geosci.* **2010**, *3*, 238−242.

(22) Schobesberger, S.; Junninen, H.; Bianchi, F.; Lönn, G.; Ehn, M.; Lehtipalo, K.; Dommen, J.; Ehrhart, S.; Ortega, I. K.; Franchin, A.; et al. Molecular understanding of atmospheric particle formation from sulfuric acid and large oxidized organic molecules. *Proc. Natl. Acad. Sci.* **2013**, DOI: 10.1073/pnas.1306973110.

(23) Curtius, J.; Lovejoy, E. R.; Froyd, K. D. Atmospheric Ion-induced Aerosol Nucleation. *Space Sci. Rev.* **2006**, *125*, 159−167.

(24) Kazil, J.; Harrison, R.; Lovejoy, E. Tropospheric New Particle Formation and the Role of Ions. *Space Sci. Rev.* **2008**, *137*, 241−255.

(25) Gagne, S.; Nieminen, T.; Kurtén, T.; Manninen, H. E.; Petäjä, T.; Laakso, L.; Kerminen, V. M.; Boy, M.; Kulmala, M. Factors influencing the contribution of ion-induced nucleation in a boreal forest, Finland. *Atmos. Chem. Phys.* **2010**, *10*, 3743−3757.

(26) Lee, S. H.; Reeves, J. M.; Wilson, J. C.; Hunton, D. E.; Viggiano, A. A.; Miller, T. M.; Ballenthin, J. O.; Lait, L. R. Particle Formation by Ion Nucleation in the Upper Troposphere and Lower Stratosphere. *Science* **2003**, *301*, 1886−1889.

(27) Zhang, R. Getting to the Critical Nucleus of Aerosol Formation. *Science* **2010**, *328*, 1366−1367.

(28) Cape, J. N.; Cornell, S. E.; Jickells, T. D.; Nemitz, E. Organic nitrogen in the atmosphere: Where does it come from? A review of sources and methods. *Atmos. Res.* **2011**, *102*, 30−48.

(29) Ge, X.; Wexler, A. S.; Clegg, S. L. Atmospheric amines - Part I. A review. *Atmos. Environ.* **2011**, *45*, 524−546.

(30) Ge, X.; Wexler, A. S.; Clegg, S. L. Atmospheric amines - Part II. Thermodynamic properties and gas/particle partitioning. *Atmos. Environ.* **2011**, *45*, 561−577.

(31) Lee, D.; Wexler, A. S. Atmospheric amines - Part III: Photochemistry and toxicity. *Atmos. Environ.* **2013**, *71*, 95−103.

(32) Schade, G. W.; Crutzen, P. J. Emission of aliphatic amines from animal husbandry and their reactions: Potential source of N2O and HCN. *J. Atmos Chem.* **1995**, *22*, 319−346.

(33) Young, L.-H.; Benson, D. R.; Montanaro, W. M.; Lee, S.-H.; Pan, L. L.; Rogers, D. C.; Jensen, J.; Stith, J. L.; Davis, C. A.; Campos, T. L.; et al. Enhanced new particle formation observed in the northern midlatitude tropopause region. *J. Geophys. Res.: Atmos.* **2007**, *112*, D10218.

(34) Qiu, C.; Wang, L.; Lal, V.; Khalizov, A. F.; Zhang, R. Heterogeneous Reactions of Alkylamines with Ammonium Sulfate and Ammonium Bisulfate. *Environ. Sci. Technol.* **2011**, *45*, 4748−4755.

(35) Qiu, C.; Zhang, R. Multiphase Chemistry of Atmospheric Amines. *Phys. Chem. Chem. Phys.* **2013**, *15*, 5738−5752.

(36) Christiansen, O.; Koch, H.; Jorgensen, P. The second-order approximate coupled cluster singles and doubles model CC2. *Chem. Phys. Lett.* **1995**, *243*, 409−418.

(37) Loukonen, V.; Kurtén, T.; Ortega, I. K.; Vehkamäki, H.; Pádua, A. A. H.; Sellegri, K.; Kulmala, M. Enhancing effect of dimethylamine in sulfuric acid nucleation in the presence of water- a computational study. *Atmos. Chem. Phys.* **2010**, *10*, 4961−4974.

(38) Nadykto, A. B.; Yu, F. Q.; Jakovleva, M. V.; Herb, J.; Xu, Y. S. Amines in the Earth's Atmosphere: A Density Functional Theory Study of the Thermochemistry of Pre-Nucleation Clusters. *Entropy* **2011**, *13*, 554−569.

(39) Pickard, F. C.; Dunn, M. E.; Shields, G. C. Comparison of model chemistry and density functional theory thermochemical

predictions with experiment for formation of ionic clusters of the ammonium cation complexed with water and ammonia; Atmospheric implications. *J. Phys. Chem. A* **2005**, *109*, 4905−4910.
(40) Pickard, F. C.; Pokon, E. K.; Liptak, M. D.; Shields, G. C. Comparison of CBS-QB3, CBS-APNO, G2, and G3 Thermochemical Predictions with Experiment for Formation of Ionic Clusters of Hydronium and Hydroxide Ions Complexed with Water. *J. Chem. Phys.* **2005**, *122*, 024302.
(41) Shields, G. C.; Kirschner, K. N. The limitations of certain density functionals in modeling neutral water clusters. *Synth. React. Inorg. Met.-Org. Chem.* **2008**, *38*, 32−36.
(42) Shields, R. M.; Temelso, B.; Archer, K. A.; Morrell, T. E.; Shields, G. C. Accurate Predictions of Water Cluster Formation, $(H_2O)_{n=2-10}$. *J. Phys. Chem. A* **2010**, *114*, 11725−11737.
(43) Temelso, B.; Phan, T. N.; Shields, G. C. Computational Study of the Hydration of Sulfuric Acid Dimers: Implications for Acid Dissociation and Aerosol Formation. *J. Phys. Chem. A* **2012**, *116*, 9745−9758.
(44) Husar, D. E.; Temelso, B.; Ashworth, A. L.; Shields, G. C. Hydration of the Bisulfate Ion: Atmospheric Implications. *J. Phys. Chem. A* **2012**, *116*, 5151−5163.
(45) Kirschner, K. N.; Hartt, G. M.; Evans, T. M.; Shields, G. C. In search of $CS_2(H_2O)$(n=1−4) clusters. *J. Chem. Phys.* **2007**, *126*, 154320.
(46) Hartt, G. M.; Shields, G. C.; Kirschner, K. N. Hydration of OCS with one to four water molecules in atmospheric and laboratory conditions. *J. Phys. Chem. A* **2008**, *112*, 4490−4495.
(47) Morrell, T. E.; Shields, G. C. Atmospheric Implications for Formation of Clusters of Ammonium and 1−10 Water Molecules. *J. Phys. Chem. A* **2010**, *114*, 4266−4271.
(48) Temelso, B.; Archer, K. A.; Shields, G. C. Benchmark Structures and Binding Energies of Small Water Clusters with Anharmonicity Corrections. *J. Phys. Chem. A* **2011**, *115*, 12034−12046.
(49) Temelso, B.; Shields, G. C. The Role of Anharmonicity in Hydrogen-Bonded Systems: The Case of Water Clusters. *J. Chem. Theory Comput.* **2011**, *7*, 2804−2817.
(50) Pérez, C.; Muckle, M. T.; Zaleski, D. P.; Seifert, N. A.; Temelso, B.; Shields, G. C.; Kisiel, Z.; Pate, B. H. Structures of Cage, Prism, and Book Isomers of Water Hexamer from Broadband Rotational Spectroscopy. *Science* **2012**, *336*, 897−901.
(51) Pérez, C.; Lobsiger, S.; Seifert, N. A.; Zaleski, D. P.; Temelso, B.; Shields, G. C.; Kisiel, Z.; Pate, B. H. Broadband Fourier transform rotational spectroscopy for structure determination: The water heptamer. *Chem. Phys. Lett.* **2013**, *571*, 1−15.
(52) Temelso, B.; Morrell, T. E.; Shields, R. M.; Allodi, M. A.; Wood, E. K.; Kirschner, K. N.; Castonguay, T. C.; Archer, K. A.; Shields, G. C. Quantum Mechanical Study of Sulfuric Acid Hydration: Atmospheric Implications. *J. Phys. Chem. A* **2012**, *116*, 2209−2224.
(53) Temelso, B.; Koddermann, T.; Kirschner, K. N.; Klein, K.; Shields, G. C. Structure and thermodynamics of $H_3O^+(H_2O)_8$ clusters: A combined molecular dynamics and quantum mechanics approach. *Comput. Theor. Chem.* **2013**, *1021*, 240−248.
(54) Case, D. A.; Darden, T.; Cheatham, T. E., III; Simmerling, C.; Wang, J.; Duke, R. E.; Luo, R.; Merz, K. M.; Pearlman, D. A.; Crowley, M. *AMBER 9*; University of California: San Francisco, 2006.
(55) Jorgensen, W.; Chandrasekhar, J.; Madura, J.; Impey, R.; Klein, M. Comparison of simple potential functions for simulating liquid water. *J. Chem. Phys.* **1983**, *79*, 926.
(56) Wang, J.; Wolf, R. M.; Caldwell, J. W.; Kollman, P. A.; Case, D. A. Development and testing of a general amber force field. *J. Comput. Chem.* **2004**, *25*, 1157−1174.
(57) Dunning, T. Gaussian-Basis Sets For Use In Correlated Molecular Calculations 0.1. The Atoms Boron Through Neon And Hydrogen. *J. Chem. Phys.* **1989**, *90*, 1007−1023.
(58) Kendall, R.; Dunning, T.; Harrison, R. Electron-Affinities Of The 1st-Row Atoms Revisited, A Systematic Basis-Sets And Wave-Functions. *J. Chem. Phys.* **1992**, *96*, 6796−6806.
(59) Xantheas, S. S. On the Importance of the Fragment Relaxation Energy Terms in the Estimation of the Basis Set Superposition Error Correction to the Intermolecular Interaction Energy. *J. Chem. Phys.* **1996**, *104*, 8821−8824.
(60) Sinha, P.; Boesch, S. E.; Gu, C.; Wheeler, R. A.; Wilson, A. K. Harmonic Vibrational Frequencies: Scaling Factors for HF, B3LYP, and MP2Methods in Combination with Correlation Consistent Basis Sets. *J. Phys. Chem. A* **2004**, *108*, 9213−9217.
(61) Merrick, J. P.; Moran, D.; Radom, L. An Evaluation of Harmonic Vibrational Frequency Scale Factors. *J. Phys. Chem. A* **2007**, *111*, 11683−11700.
(62) Johnson, R. D.; Irikura, K. K.; Kacker, R. N.; Kessel, R. É. Scaling Factors and Uncertainties for ab Initio Anharmonic Vibrational Frequencies. *J. Chem. Theory Comput.* **2010**, *6*, 2822−2828.
(63) Diri, K.; Myshakin, E. M.; Jordan, K. D. On the Contribution of Vibrational Anharmonicity to the Binding Energies of Water Clusters. *J. Phys. Chem. A* **2005**, *109*, 4005−4009.
(64) Dunn, M. E.; Evans, T. M.; Kirschner, K. N.; Shields, G. C. Prediction of Accurate Anharmonic Experimental Vibrational Frequencies for Water Clusters, $(H_2O)_n$, n=2−5. *J. Phys. Chem. A* **2006**, *110*, 303−309.
(65) Barone, V. Vibrational Zero-point Energies and Thermodynamic Functions Beyond the Harmonic Approximation. *J. Chem. Phys.* **2004**, *120*, 3059−3065.
(66) Truhlar, D. G.; Isaacson, A. D. Simple Perturbation Theory Estimates of Equilibrium Constants from Force Fields. *J. Chem. Phys.* **1991**, *94*, 357−359.
(67) Frisch, M. J.; Trucks, G. W.; Schlegel, H. B.; Scuseria, G. E.; Robb, M. A.; Cheeseman, J. R.; Montgomery, J. A.; Vreven, T.; Kudin, K. N.; Burant, J. C.et al. *Gaussian 09*, revision B.02; Gaussian, Inc.: Wellington, CT, 2009.
(68) Pettersen, E. F.; Goddard, T. D.; Huang, C. C.; Couch, G. S.; Greenblatt, D. M.; Meng, E. C.; Ferrin, T. E. UCSF chimera - A visualization system for exploratory research and analysis. *J. Comput. Chem.* **2004**, *25*, 1605−1612.
(69) Neese, F. The ORCA program system. *Wiley Interdiscip. Rev.: Comput. Mol. Sci.* **2012**, *2*, 73−78.
(70) Robertson, W. H.; Johnson, M. A. Caught in the act of dissolution. *Science* **2002**, *298*, 69.
(71) Gutberlet, A.; Schwaab, G.; Birer, Ö.; Masia, M.; Kaczmarek, A.; Forbert, H.; Havenith, M.; Marx, D. Aggregation-Induced Dissociation of HCl(H2O)4 Below 1 K: The Smallest Droplet of Acid. *Science* **2009**, *324*, 1545−1548.
(72) Forbert, H.; Masia, M.; Kaczmarek-Kedziera, A.; Nair, N. N.; Marx, D. Aggregation-Induced Chemical Reactions: Acid Dissociation in Growing Water Clusters. *J. Am. Chem. Soc.* **2011**, *133*, 4062−4072.
(73) Relph, R. A.; Guasco, T. L.; Elliott, B. M.; Kamrath, M. Z.; McCoy, A. B.; Steele, R. P.; Schofield, D. P.; Jordan, K. D.; Viggiano, A. A.; Ferguson, E. E.; et al. How the Shape of an H-Bonded Network Controls Proton-Coupled Water Activation in HONO Formation. *Science* **2010**, *327*, 308−312.
(74) Leopold, K. R. Hydrated Acid Clusters. *Annu. Rev. Phys. Chem.* **2011**, *62*, 327−349.
(75) Rozenberg, M.; Loewenschuss, A. Matrix Isolation Infrared Spectrum of the Sulfuric Acid, Monohydrate Complex: New Assignments and Resolution of the Missing H-Bonded (OH) Band,Issue. *J. Chem. Phys.* **2009**, *113*, 4963−4971.
(76) Zatula, A. S.; Andersson, P. U.; Ryding, M. J.; Uggerud, E. Proton mobility and stability of water clusters containing the bisulfate anion, HSO4-(H2O)n. *Phys. Chem. Chem. Phys.* **2011**, *13*, 13287−13294.
(77) Erupe, M. E.; Benson, D. R.; Li, J.; Young, L.-H.; Verheggen, B.; Al-Refai, M.; Tahboub, O.; Cunningham, V.; Frimpong, F.; Viggiano, A. A.; et al. Correlation of aerosol nucleation rate with sulfuric acid and ammonia in Kent, Ohio: An atmospheric observation. *J. Geophys. Res.: Atmos.* **2010**, *115*, D23216.
(78) Yu, H.; Lee, S. H. Chemical ionisation mass spectrometry for the measurement of atmospheric amines. *Environ. Chem.* **2012**, *9*, 190−201.
(79) Ortega, I. K.; Kupiainen, O.; Kurten, T.; Olenius, T.; Wilkman, O.; McGrath, M. J.; Loukonen, V.; Vehkamaki, H. From quantum

chemical formation free energies to evaporation ratesRID A-7930−2008. *Atmos. Chem. Phys.* **2012**, *12*, 225−235.
(80) Kupiainen, O.; Ortega, I. K.; Kurtén, T.; Vehkamäki, H. Amine substitution into sulfuric acid−ammonia clusters. *Atmos. Chem. Phys.* **2012**, *12*, 3591−3599.
(81) Olenius, T.; Kupiainen-Maatta, O.; Ortega, I. K.; Kurten, T.; Vehkamaki, H. Free energy barrier in the growth of sulfuric acid–ammonia and sulfuric acid–dimethylamine clusters. *J. Chem. Phys.* **2013**, *139*, 084312.
(82) Xu, W.; Zhang, R. A theoretical study of hydrated molecular clusters of amines and dicarboxylic acids. *J. Chem. Phys.* **2013**, *139*, 064312.
(83) Bzdek, B. R.; Ridge, D. P.; Johnston, M. V. Amine reactivity with charged sulfuric acid clusters. *Atmos. Chem. Phys.* **2011**, *11*, 8735−8743.